N93-29724

ADVANCED DESIGN FOR ORBITAL DEBRIS REMOVAL IN SUPPORT OF SOLAR SYSTEM EXPLORATION

UNIVERSITY OF ARIZONA

5/2-18
160588
p. 7

The development of an Autonomous Space Processor for Orbital Debris (ASPOD) is the ultimate goal of this project. The craft will process, *in situ*, orbital debris using resources available in low Earth orbit (LEO). The serious problem of orbital debris is briefly described and the nature of the large debris population is outlined. This year, focus was on development of a versatile robotic manipulator to augment an existing robotic arm; incorporation of remote operation of robotic arms; and formulation of optimal (time and energy) trajectory planning algorithms for coordinating robotic arms. The mechanical design of the new arm is described in detail. The versatile work envelope is explained showing the flexibility of the new design. Several telemetry communication systems are described which will enable the remote operation of the robotic arms. The trajectory planning algorithms are fully developed for both the time-optimal and energy-optimal problem. The optimal problem is solved using phase plane techniques while the energy optimal problem is solved using dynamics programming.

INTRODUCTION

The problems presented by orbital debris have been gaining attention in recent years. Science writers[1-4] and the popular news media[5-9] have lucidly described these problems. The orbital debris problem merited a report from the General Accounting Office[10] describing the threats to future space stations and other space operations. The Advanced Design team at the University of Arizona continues to develop a spacecraft that will economically remove the large debris through local resource utilization. The fundamental idea is to concentrate solar energy into a point-focus and cut the debris into precise shapes that the robotic arms can assemble into a manageable configuration. After having processed several debris pieces three disposal modes exist: (1) retrieval by the shuttle; (2) precise splashdown into the oceans; or (3) planned burn-up during atmospheric reentry.

A study conducted by the University of Arizona in 1989 showed that there were 386 objects in Earth orbit that qualify as large debris (mass 1,500 kg). Each object included in this list has a sufficient orbital lifetime to ensure its existence past the year 2000. This study also identified several specific orbital inclinations where a majority of the large debris exists (Fig. 1).

Mission feasibility studies have shown that one Autonomous Space Processor for Orbital Debris (ASPOD) could process at least five of the large pieces of debris with reasonable propellant requirements[11]. This is accomplished by taking advantage of nodal regression differences and through the use of classic Hohmann transfers.

This year's work focused on the development of a versatile robotic manipulator, investigation of remote operation of the existing solar collector and a new robotic arm, and the formation of trajectory planning algorithms for coordinated robotic arms carrying a common object. This report is a summary of the work.

This year, five new students were involved in the ASPOD design. Four were involved with design and fabrication of a robotic manipulator, while the other student refined the solar tracking device and investigated telemetry systems for future use. In addition, two local high school students were actively involved in the project.

Since the launch of Sputnik in 1957, satellites have orbited the Earth, completed their missions, then burned upon reentry into the atmosphere. Unfortunately, it sometimes takes decades to complete this last step. Three decades into the space age, the amount of junk orbiting the Earth has mushroomed. It includes everything from long-dead satellites, which outnumber working satellites[1], to rocket boosters, clamps, satellite shields, explosive bolts, and even sewage.

Space pollution poses a number of problems. Orbital debris creates a collision hazard for manned and unmanned spacecraft. Defunct satellites falling from orbit, especially those with nuclear power sources, imperil everyone on the ground. Ground-based astronomers already have had observations marred by light reflected from satellites and other orbiting chunks of material passing in front of telescopes[2].

The problem of collision with orbital debris is much more severe than most people imagine. At orbital velocities (typically 7-10 km/s) in LEO, a 1-g mass possesses the same kinetic energy

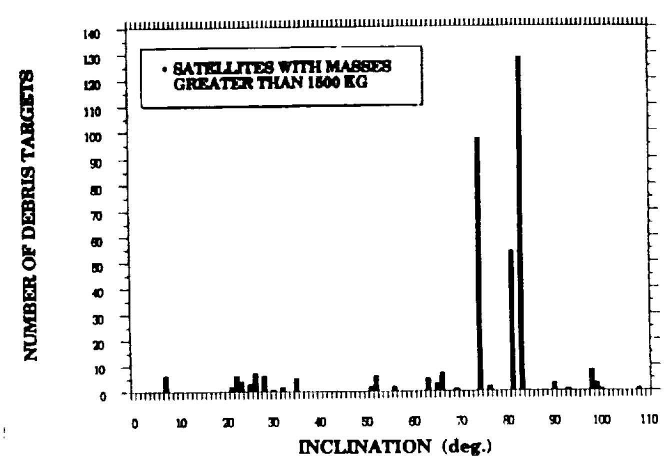

Fig. 1. Inclination where large debris population exists.

as a 50-g bullet travelling at 3300 ft/s (approximately 1000 m/s); a more easily understood analogy is that a 25-g piece of orbital debris in LEO possesses the same energy as a 3000-lb automobile travelling at 60 mph[3]. The large pieces of junk (dead satellites, and rocket boosters) are not the immediate problem. They are easily trackable by radar and avoided by manned and manned spacecraft. The real problem occurs when these large pieces collide with each other, becoming many thousands of smaller, untrackable, and potentially disastrous projectiles. Excerpts from recent letter written by Dr. Kumar Ramohalli of the University of Arizona, address some of the misconceptions of the orbital debris problem.

> Several myths have been propagated regarding orbital debris. (1) The millions of smaller pieces pose a hazard: the eight thousand or so larger ones are not hazardous and can be avoided. [The truth is that these large ones, left alone can create innumerable smaller ones through collisions; we had better remove them while they are still trackable.] (2) Space debris is likely to become a major problem only after 2000 A.D. Why waste our resources trying to build spacecraft to mitigate the future hazards? [The truth is it takes a minimum of ten years to conceptualize, design, fabricate, test and qualify any spacecraft. So the time to start is now.] (3) We know so little about space debris that many more studies are needed for characterization; retrieval can wait. [The truth is that there exists an extensive data bank, continuously updated, on the larger debris. In fact we even have their trajectories, geometry, mass, and sometimes even the remaining propellant in them.]
>
> We could go on, but the point should be clear. These stalling arguments can only be interpreted as a general lack of interest in accepting a problem that is growing at an alarming rate. Don Kessler's own estimates show that space operations could become very hazardous by 2010.
>
> We have approached various authorities, including DoE, DoD who are interested in toxic waste clean-up here on Earth. An autonomous robot that is equipped with solar furnaces and pattern recognition capabilities, image processing, digital filtering, and *in-situ* chemical processing can be sent terrestrially to hazardous waste sites and will detoxify the wastes. Thus, the space-derived technologies may have more immediate applications here on Earth too.

Dr. Ramohalli has proposed using solar energy to process these large pieces of debris, making disposal or reclamation easier. A solar focal-point metal cutter will focus the Sun's energy to a point with an intensity great enough to cut the material. The ASPOD prototype currently consists of a solar powered metal cutter mounted on a wheel table that has been fitted with a telescope equatorial mount to maintain focus of the Sun. One robotic arm has been designed and built to operate satisfactorily with the ASPOD prototype. The space-based unit will need two arms to insure that the final movement imparted to the debris will not cause the severed piece to move toward the fragile lenses and mirrors of the metal cutter.

ROBOT MANIPULATOR ARM

Design requirements for the robot manipulator arm call for a rather large working envelope. The arm must be able to retrieve the target debris at a safe distance; it must manipulate the debris at the focal point, position cut pieces near the mirrors, and stow unusable pieces in the storage bin. For the one-fifth scale prototype a stationary robot would need a reach of over ten feet. This year's design team developed a six-degree-of-freedom robotic arm with the additional feature of a mobile mount that reduced the necessary length of each segment. Upon assembly and testing, the robotic arm satisfied all design specifications.

DESIGN OF THE MOBILE MOUNT

The mobile mount is a rotating base for a manipulator. The base is designed to maximize the working envelope of the manipulator arm while minimizing its length and weight requirements.

A top view of the mount is shown in Figs. 2 and 3. The power needed for the mobile mount comes from a parallel shaft TENV gear motor, which is geared down before driving the shaft that goes through the ASPOD platform. The shaft is supported by ball bearings and drives an arm that sits on shoulders machined into the shaft. The other end of the arm rotates with the shaft, thus providing the mobility. The manipulator will "ride" on the far end of the arm near the guide wheel assembly. The guide wheel assembly prevents the arm from moving normal to the ASPOD platform as well as resisting torsional twisting. The arm is guided by a track that is attached to the ASPOD platform.

SHAFT ASSEMBLY

The center point of the mobile mount assembly is the central shaft. This shaft supports the torque generated by the weight of the manipulator. The maximum torque, as defined by the static and dynamic model of the manipulator, is approximated at 55 lbf-ft. Carbon steel was the material chosen for the shaft because of its relatively high modulus of rigidity and its availability. The diameter chosen for this design was 1.5 inch. A 13.5 × 14.5-in steel plate supports the shaft. This material was chosen for its high strength and availability. The plate was mounted beneath the ASPOD platform, secured by half-inch bolts to the metal frame of the platform. SKF Industries, Inc. #FY 1 1/2 TM bearings were used to support the shaft. These bearings support both radial and axial loads and are relatively low in cost. The bearings make a sandwich around the steel plate thus supporting the shaft (see Figs. 2 and 3).

MOBILE ARM AND WHEEL GUIDE ASSEMBLY

The primary considerations in the design of the mobile arm were: (1) attachment to the central shaft, (2) torsional deflection under the maximum calculated load, and (3) attachment to the wheel guide assembly. A 1.5-in central shaft extends from the top of platform. The maximum torque on the arm was calculated at 650 lb/in. The wheel guide assembly will be mounted to 6061-T6 1.5-in square stock. With these considerations in mind, the arm was designed and fabricated out of 2 × 5 rectangular aluminum (wall thickness = 3/16 in) which was determined to satisfy the design requirements. The machining modifications are shown in Figs. 2 and 3. The wheel guide assembly is responsible for supporting the mobile arm vertically as well as resisting torsional twisting. It was determined that four 6200 series double shield ball bearings will be supported by 10 × 40-mm grade-8 bolts mounted in adjustable supports machined from 6061-T6 aluminum stock. Hardware

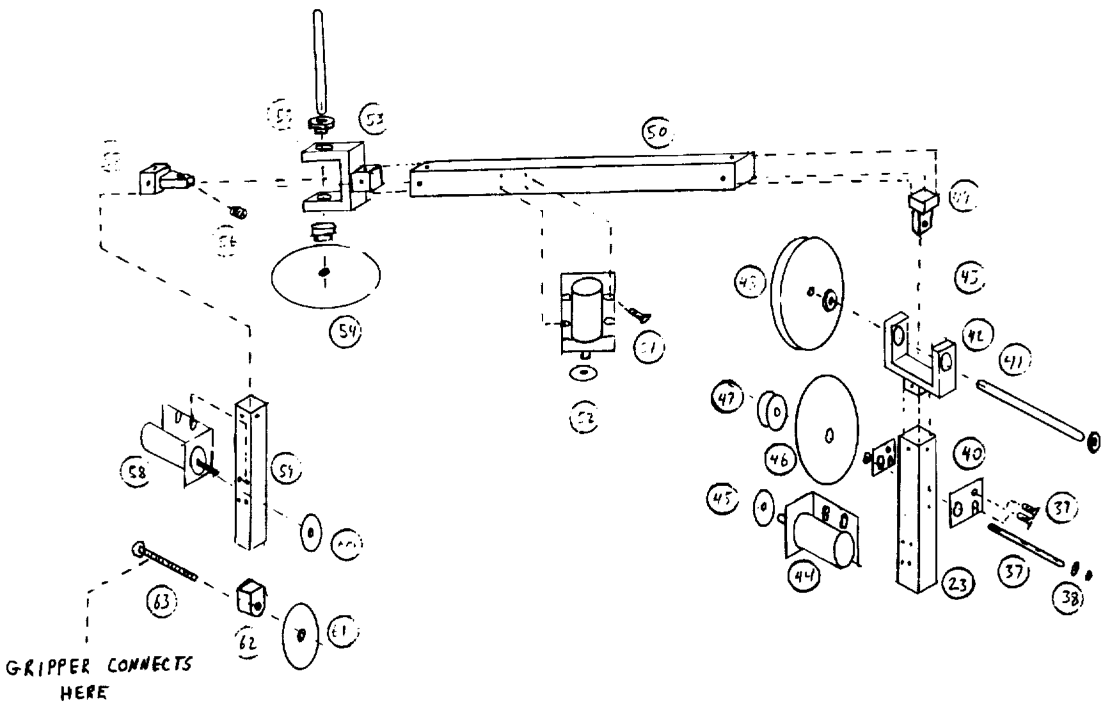

Fig. 2. Manipulator Components.

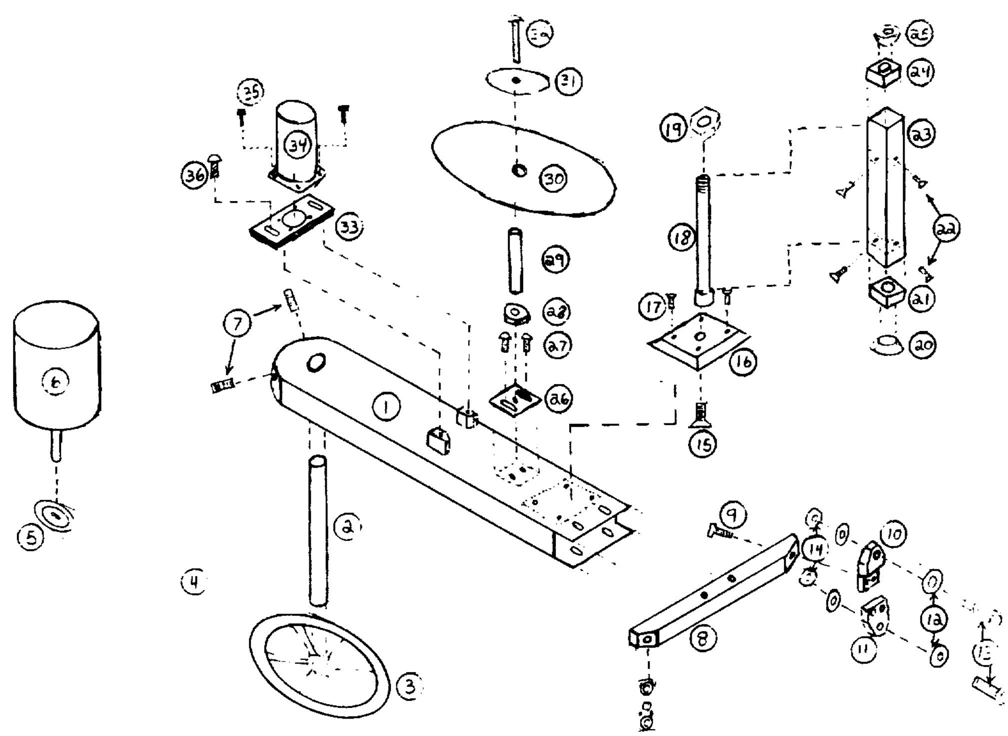

Fig. 3. Rotation Assembly.

is shown in Figs. 2 and 3. After assembly, testing indicated that all components performed as designed. There was no measurable deflection at the wheel/track interface or at the shaft/arm interface.

TRACK AND TRACK MOUNTS

For the mobile arm, a track was required to allow for movement from one side of the ASPOD platform to the other. The track needed to allow for a guide wheel assembly that would resist motion perpendicular to the mobile mount. After much consideration we decided to use a piece of 3/16-in cold-rolled steel, 2 1/2 in wide. The piece of steel, approximately 12 ft long, was formed into a 5-ft-diameter circle. The track was then mounted to a piece of 3/4-in plywood, which was mounted to the ASPOD platform. In mounting the track to the ASPOD platform, we needed a mount that would allow for complete motion of the mobile arm on the inner diameter of the track. To do this, 3/8-in holes were drilled every 6 inches in the track. A 3/8 × 2-in allen cap screw was used to mount the track to a 4 × 4-in piece of angle that was mounted to the plywood platform. This mounting system for the mobile arm guide wheel assembly allows for the complete motion of the mobile arm in the inner diameter of the track and would also allow no motion perpendicular to the mobile mount.

MANIPULATOR LINK AND JOINT MATERIAL

After consideration of various materials the decision was made to use aluminum alloy 6061-T6 for the construction of the manipulator links and joints. This alloy, which contains both magnesium and silicon, was chosen because of its good formability, machinability, weldability, and its good corrosion resistance. The temper designation, T6, means this alloy has been solution treated and artificially aged. The major reason for its selection was its relative availability and low cost compared to the other materials considered. Table 1 lists some of the important physical and mechanical properties.

DEFLECTION AND MOMENT ANALYSIS

The manipulator links will be numbered I, II, and III, beginning at the mobile mount and moving toward the free end of the arm. The shape and dimensions of each link were chosen by using a combination of the availability of a particular material shape and the minimum size needed to attach the necessary actuators to the link's end. Table 2 shows the dimensions of the links. All links are hollow square tubes enabling the routing of wires through their centers.

Using these dimensions, a deflection analysis was performed to make certain that these links would meet the specification of a maximum deflection of 1 cm (0.39 in). This is defined as the difference in deflection between the loaded link and the unloaded link. It will be assumed that the unloaded link will have a 100% repeatability in positioning. Then, if the loaded link can be positioned within 0.39 in. of the unloaded link, the specification will be considered satisfied. A rough schematic of the assembled manipulator can be seen in Fig. 4. The dimensions shown are those dimensions necessary for a deflection and torque analysis. The deflection results are listed in Table 3.

TABLE 1. Al 6061-T6 Properties.

Properties	Units	Value
Yield Strength	kpsi	40
Ultimate Strength	kpsi	45
Modulus of Elasticity	10^6 psi	10.3
Modulus of Rigidity	10^6 psi	3.8
Density	lbs/in^3	0.098
Strength to Weight Ratio	10^6 in	105.1

TABLE 2. Link Dimension.

Link	Dimension (in)	Weight (lb)
I (square)	2 × 2 1/8 × 12	1.1
II (square)	2 × 2 1/8 × 24	2.2
III (square)	2 × 2 1/8 × 12	1.1

As is evident from the difference values in Table 3, the chosen link dimensions fully meet the deflection design specifications. Using these links, the moments developed at the attached end of each link were calculated. The results from calculations for loaded and unloaded can be seen in Table 4.

These values are important because they can be translated into torque requirements for the actuators between the links if one considers static conditions only. It is obvious that any final torque values must contain dynamic as well as static requirements. The equation for the Lagrangian method (1) for determining torque clearly shows that the torque is

$$\tau = (ml_c^2 + I)\theta + mgl_c\cos(\ddot{\theta}) \qquad (1)$$

the sum of the potential energy (static) and the kinetic energy (dynamic) terms. The necessary torques can be calculated from (1) ignoring the kinetic energy term if the angular acceleration can be kept several orders of magnitude less than the potential energy acceleration term "*g*". This will result in a situation where only static conditions will be necessary to calculate torques. By investigating Fig. 5, it is clear that if the time frame can be kept below 30 seconds, torque values can be established by considering static requirements alone, as the angular acceleration term will result in a dynamic value several orders of magnitude less than the static term.

The time in this figure will be the time required to move the link from a vertically down position to a vertically up position. An angular velocity of 1/2 rpm corresponds to a time of 30

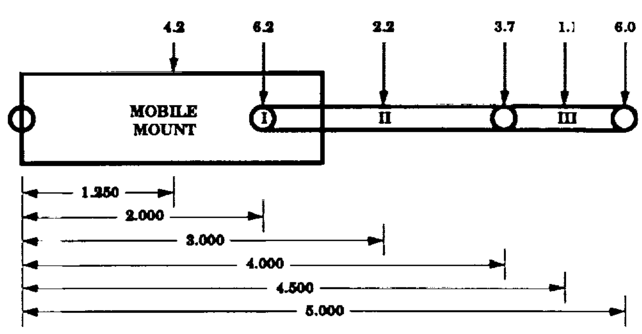

Fig. 4. Deflection and Torque Parameters.

TABLE 3. Link Deflections.

Link	Unloaded (in)	Loaded (in)	Difference (in)
I	0.0054	0.0054	<0.0001
II	0.0134	0.0135	0.0001
III	0.0006	0.0007	0.0001

TABLE 4. Link End Moment Requirement.

Link	Unloaded (lb-in)	Loaded (lb-in)	Difference (lb-in)
I	285.61	287.11	1.50
II	285.61	287.11	1.50
III	78.60	79.35	0.75
Mobile Mount	888.0	891.75	3.75

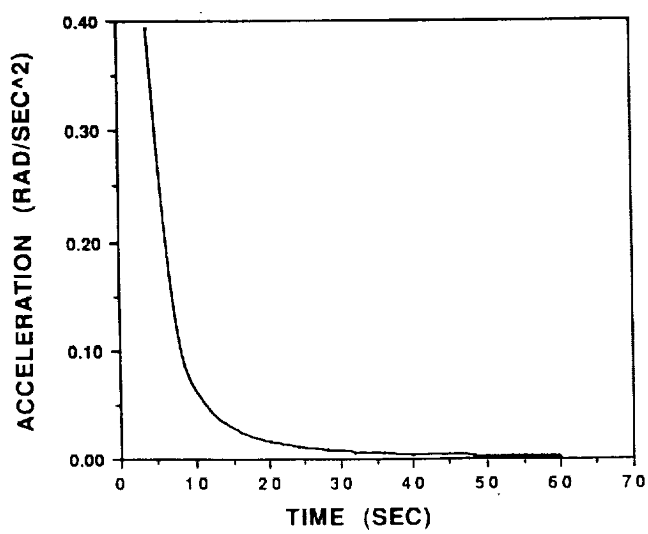

Fig. 5. Acceleration Requirements.

sec, and it is clear that this time-frame is approximately the point where the acceleration begins to rise very rapidly. It is clear that if the angular velocity can be kept at 1/2 rpm or lower, the Lagrangian equation can be solved to a high degree of accuracy while considering only the static or potential energy term alone. The Langrangian equation shows the difficulty in representing on Earth a manipulator designed for space. On Earth, the dominant acceleration term is gravity. As shown, this is at least four times the magnitude of the angular acceleration term. However, in orbit this gravity term will be zero and angular acceleration will be the controlling parameter regardless of how small it might be.

JOINTS AND ACTUATORS

To join the manipulator, links together it was necessary to manufacture joints that allow the required degrees of freedom for each link. The joints are fashioned similar to a yoke, as shown in Fig. 2 (*42 and 53) are made of 6061-T6 aluminum. The shaft is connected to the female portion of the yoke by antifriction radial bearings, which also is connected to the male portion of the yoke as shown in Fig. 2. For the rotary motion, a sprocket set is used in conjunction with a DC motor. For the motion between links I and II a double sprocket pair is used. For the motion between links II and III a single sprocket pair is used. The motors are connected to the links by means of a mount, also shown in Fig. 2.

The torque required for the joint connecting links I and II is 4569.6 oz-in and 1257 oz-in for the joint connecting links II and III. The torques were calculated as for the manipulator links. For links I and II a double sprocket pair with a reduction of 16:1 was used. This resulted in the required torque at the motor to be 285.6 oz-in. A permanent-magnet DC gear head motor with a maximum torque of 400 oz-in was used, giving a safety factor of 1.4 at maximum load. For links II and III a single sprocket pair with a reduction of 6:1 was used. This resulted in the required torque at the motor to be 209.6 oz-in. A permanent-magnet DC gear head motor with a maximum torque of 400 oz-in was also used, resulting in a safety factor of 1.9 at maximum load.

WRIST AND GRIPPER

The wrist assembly is designed to provide bending and rotational motion for the gripper. Bending motion is provided by the rotation of a 200 oz-in DC gear head motor. As shown in Fig. 2, a shaft connected to the gripper controls its rotational motion. This shaft is supported by two ball bearings positioned in a gripper end-block machined from solid aluminum. The shaft is driven by a 3:1 ratio sprocket pair connected to the motor. A 3.5-in extension piece connects the shaft to the supporting collar. This moves the rotation point closer to the center of gravity so the demands on the motor are reduced. With the extension piece and sprocket pair, there is a safety factor of 4.7 on this motor.

Rotational motion is provided by a DC motor connected directly to the gripper. The output shaft of the motor rotates a 1/4-in shaft that extends through a supporting collar. The supporting collar is a hollow aluminum piece that encases two ball bearings with a 1/4-in inner diameter. This shaft is rigidly attached to the housing for the push/pull motor, which controls the gripper (Fig. 3).

The gripper was adapted from a manipulator that is no longer functional. It is solid aluminum with a series of 1/4-in holes drilled through the solid part of the gripper to reduce weight. The gripper weighs 2.0 lb. A push/pull motor encased in the lower part of the gripper controls the gripper action. Figure 3 shows this assembly.

TELEMETRY

The telemetry system for the ASPOD is designed to control the robotic arm and to simulate future operation of the system in space. A few telemetry subsystem requirements are:

- A duplex communication link (i.e., a transmitter and a receiver at both remote and local sites)
- A self-contained power source for the system on the remote end
- Real time operation
- Redundancy (for space application)

Taking these factors into account, a Radio Modem and a Photonic telemetry system were chosen for evaluation.

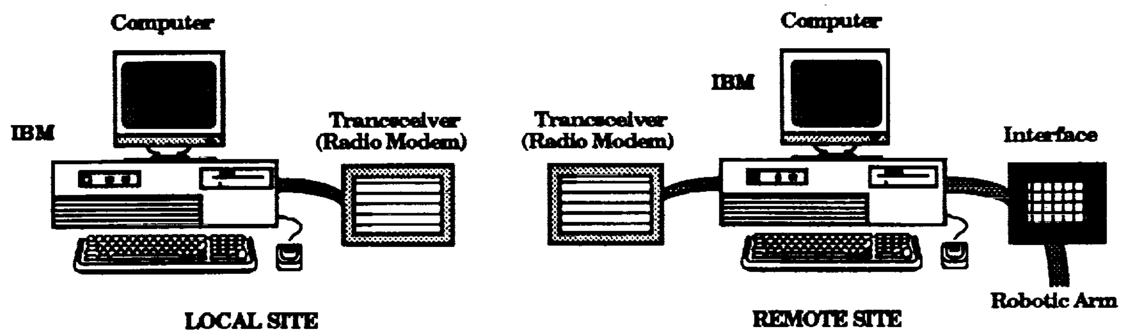

Fig. 6. 1991-1992 Radio Modem Telemetry System.

Telemetry Systems

The Radio Modem telemetry system (see Fig. 6) is composed of a lap-top IBM PC connected to a transceiver (radio modem) and an interface at the remote site. At the local (user) site an IBM PC is connected to a transceiver. The computers are linked to the modems with an RS-422 serial port.

To simulate the telemetry system to be used in space, a self-contained power source (for the remote site) has been proposed. Wires will connect the computer and modem, the computer and interface, and the power source to the computer and modem. The power source to be used is solar energy.

Likewise, the Photonic telemetry system uses local resources to operate. This system is an optical-pulse-powered sensor system that converts an incoming optical pulse (or a series of pulses) to a voltage by an array of photovoltaic cells. There is no external power source required for the (remote) sensing end. This system improves the performance of the conventional two-wire electronic telemetry system because there are fewer electronic components, and therefore less heat to be dissipated. Additionally, this system isolates the electronic components, which reduces the electromagnetic interference (EMI) between links of the beam.

Both Radio Modem Optical Link telemetry systems have duplex communication links, a self-contained power source (for the remote end), and operate in real time. Redundancy could be applied, but it is only needed for space application. Nevertheless, there are disadvantages to each system. A direct line-of-sight must be maintained for both systems. This requirement is not as strict for the Radio Modem telemetry system as for the Photonic telemetry system. However, once a direct line-of-sight is achieved for the laser, the signals through radio frequency (RF) waves will fade occasionally (throughout the month) due to sunspots.

ASPOD Telemetry System

The Radio Modem telemetry system will be used for ground application on the ASPOD project. It will still simulate space operation by having a self-contained power source and radio frequency (RF) shield (for each part of the system) to block out radio frequency interference (RFI). However, the Photonic telemetry system should be incorporated into the future design for space application. The final system will need a radiation shield to minimize RFI.

Solar Tracker

A solar tracking system was designed to use the Sun's energy to cut orbital debris. For this system to work effectively as well as efficiently, the ASPOD solar cutter must be directly aligned with the Sun (in elevation and azimuth) to obtain a maximum amount of solar energy. This alignment is required to focus energy to a point faster than it can be conducted, convected, reflected, emitted, or radiated away[1]. The solar tracking system is composed of two directional systems (one for elevation and the other for azimuth), and a control box. Within each directional system is mounted gear train apparatus, a 90-V DC motor, and a pair of solar photovoltaic cells.

Solar Photovoltaic Cells

The solar photovoltaic cells are arranged in right-angled configurations. These sensors are mounted on the ASPOD with the bisector of the angle between the cells perpendicular with the focal axis of the solar cutter. Depending on which solar cell is receiving the most solar flux, a voltage difference (positive or negative) will result. However, if the solar flux is of equal intensity on each solar cell, the voltage difference will be zero. This voltage output is sent to the control box which then sends a signal to the servo motor. Note that the two directional systems are independent of each other.

The voltage is related to the direction of the solar tracker in the following manner: If the voltage difference across the solar cells is zero, the solar tracker is in direct alignment with the Sun; if there is a positive or negative voltage difference, then the tracker is leading or lagging the Sun.

ACKNOWLEDGEMENTS

Summary report prepared by Dr. Kumar Ramohalli and Micky Marine, James Colvin, Richard Crockett, Lee Sword, Jennifer Putz, Sheri Woelfle. The support from USRA and technical monitoring of Mr. James D. Burke of JPL are gratefully acknowledged. We also would like to thank Mr. Milton Schick who contributed toward the new robotic arm.

REFERENCES

1. Beard, Jonathon. *Sweeping Up Space Junk,* Discovery, December 1988, p.22.
2. Lechleitner, Hans. *Raumpfleger Dringend Gesucht,* March 1989, p154. Geo in German
3. Beard, Jonathon. *Verdens Forste Flyvende Skraldemand,* Danish Science, December 1988, p46.
4. Stewart, Doug. *Eyes in Orbit Keep Tabs on the World in Unexpected Ways,* Smithsonian, December 1988, p70.
5. Erickson, Jim. *Engineer Plans to Clean the Heavens,* Arizona Daily Star, February 21, 1987.
6. Stiles, Edward. *Space Junk,* Tucson Citizen, February 27, 1987.
7. Hodge, Carl. *'Sweeper' Would Gather Space Debris,* Arizona Republic, August 14, 1988.
8. Stiles, Edward. *U of A Robot Will Collect Space Junk,* Tucson Citizen, September 23, 1988.
9. Turner, Mark Holman. *Trashed in Space,* American Way, May 15, 1989.
10. *General Accounting Office Report,* April 1989.
11. Ramohalli, Kumar, et al. *Autonomous Space Processor For Orbital Debris,* USRA Summer Conference, June 12, 1989.